A linear Stirling cooler for extreme ambient temperatures

D. Willems, J. Mullié, F. v. Wordragen, G. de Jonge

Thales Cryogenics B.V., Eindhoven, The Netherlands

ABSTRACT

With the achievements made in the last decade with respect to reliability and cryogenic performance, the use of linear cryocoolers for new application areas has become viable. Thales Cryogenics has been challenged by its customers to deliver robust and compact solutions for a variety of applications.

One of these challenges is the use of coolers in extreme environmental conditions. In this paper, a linear Stirling cooler is presented that is designed for use in such extreme conditions, one of which is an ambient temperature of 150°C. The application for which this cooler is intended - the cooling of electronics and imaging sensors – requires 25 W of cooling power between 423 K and 223 K. Because of the need for a high-efficient solution within a limited geometrical envelope, a Stirling cooler was selected as the most suitable cooler type.

We will describe the impact of the high ambient temperatures on the fundamental thermodynamics of the Stirling cooler. Furthermore, we will present some of the practical challenges in the design of the cooler. Finally, we will present the results of the qualification and performance testing of the coolers that were built.

INTRODUCTION

Linear cryocoolers have been in use for a large range of applications. Traditionally, Stirling coolers are used for sensing applications such as infrared systems. In these tactical applications, harsh environmental conditions, both thermal and mechanical, are combined with an increasing demand in reliability. Likewise, pulse-tube coolers with flexure-bearing compressors are used in situations where reliability is even more important, such as space applications.

The resulting combined knowledge in the design and testing of coolers has enabled Thales Cryogenics to meet the challenging requirements of its customers in all sorts of applications [1]. One such application is described in this paper. For an application in the petrochemical industry, in-situ inspection of oil wells, a cooling solution was required. The inspection tool uses sensors and electronics that need sub-ambient temperatures for correct functioning, while the environment in which these systems operate have an increasingly high environmental temperature. Because of the depletion of oil reserves near the earth's surface, oil wells are increasingly further below the surface with the associated increase of temperature due to geothermal influence.

Figure 1: Photograph of two of the coolers.

Off shore test equipment also requires severe mechanical robustness because of the handling of the equipment and the down-hole use. Finally, the solution needs to be compact because of the limited available space envelope in the cylindrical measurement tools.

The cooling requirement was a cooling power of 25 W at tip temperature of 223 K, with an environmental temperature of 423 K. The application did not allow the use of 'non-cryogenic' technology such as vapor compression or thermo-electric. Therefore, a mechanical cooler of the Stirling or pulse-tube type was needed.

In this paper, the trade-offs in cooler type and design choices are presented. Also the impact of the environmental temperatures is further described. Furthermore, the qualification and test results of the first cooler batches are presented.

COOLER TYPE TRADE-OFF

There was no initial preference for either a Stirling or pulse-tube cooler. A trade-off had to be made based on the criteria of efficiency, size, and robustness.

The theoretical maximum efficiency of a cooler is different for a Stirling and pulse-tube cooler. For a Stirling cooler the theoretical maximum efficiency is that of Carnot, for a pulse tube it is the ratio between cold and hot end temperatures.

For the two coolers, the theoretical maximum efficiency is shown in Figure 1below. In comparison with cryogenic applications, the temperature difference is the same, while the absolute temperatures are higher. As a consequence, the theoretical maximum efficiency increases more for the Stirling cooler. This means that the theoretical maximum efficiency in this case is approximately twice to four times higher for the Stirling cooler. Practical efficiencies will be a lot lower, but it is still to be expected that the actual efficiency difference will show a similar trend.

There is also a size and mass advantage, as a Stirling cooler typically has a lower system volume per watt of cooling power. This is due to the absence of the inertance tube and buffer, as well as the larger required swept volume for the same PV power. So it is expected that also for this case, the Stirling cooler will have a smaller overall size. In the application, the cooler needed to fit within a defined cylindrical envelope.

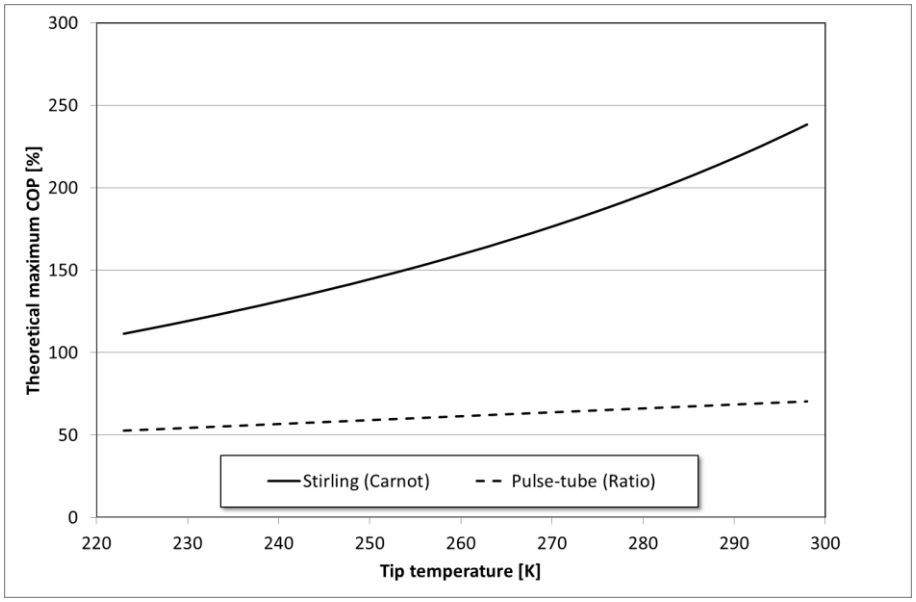

Figure 2: Theoretical maximum efficiency versus tip temperature at 150°C hot end temperature for Stirling and pulse-tube coolers. For Stirling coolers this is the Carnot efficiency, for a pulse tube the ratio between hot and cold-end temperatures.

In terms of reliability and robustness, the pulse-tube cooler is the better choice. However, in this application the high life time of a pulse tube is not required; the number of cooler operating hours within the system life time is low, so there is no clear advantage to the inherent robustness and reliability of the pulse-tube cold finger.

Based on the high efficiency and lower system volume, the cooler type of choice for this cooler is the Stirling cooler.

DESIGN DETAILS

Thermodynamic design

The detailed thermodynamic design of the cooler was done using both SAGE and Thales' proprietary Stirling simulation tools. The optimization of the cold finger and compressor was done consecutively to ensure both maximum thermodynamic efficiency and compressor efficiency.

It was found that the optimum cold finger geometry was very close to the existing LSF9340 Stirling cold finger. The latter is optimized for thermodynamic efficiency at 80 K. To enable the use of existing tools and equipment as much as possible, the overall geometry of the parts was kept equal as much as possible, while details such as regenerator matrix and tuning of the free displacer were optimized specifically for this temperature range.

Because of the higher gas temperatures, the gas density is lower than in typical cryogenic applications. The irreversible losses in the cooler are the sum of heat transfer losses, heat conduction losses, and viscous losses. In [2], the following equation is given for the entropy production per unit of regenerator volume,

$$\sigma_i = \beta \frac{(T_r - T_g)^2}{T_r T_g} + \frac{\lambda_g}{T_g^2}\left(\frac{\partial T_g}{\partial x}\right)^2 + \frac{\lambda_r}{T_r^2}\left(\frac{\partial T_r}{\partial x}\right)^2 + \frac{\eta z (jV_m)}{T_g}. \quad (1)$$

It shows 4 different contributions to the overall entropy production. The first term is the losses due to finite heat transfer, determined by the heat transfer coefficient β and matrix and gas temperatures T_r and T_g. The second and third parts are the contributions of heat conduction through the gas and matrix respectively. These are proportional to the thermal conductivity λ and the temperature gradient. The fourth term is the loss due to flow resistance, proportional to the

viscosity η, flow impedance factor z, and volume flow rate (molar flow j times molar volume V_m).

In a coarse approximation it can be seen that, with increasing temperature, all terms will reduce because of the temperature terms in the denominators. However, the flow resistance term will increase less. This means that the contribution of flow resistance to the total entropy production in the regenerator will become more dominant. This leads to a different regenerator optimization compared to coolers for lower temperatures. As a consequence, due to the relation between pressure drop and driving force of the displacer, the displacer dynamics also needs to be tuned differently.

Design challenges

Apart from the different trends in thermodynamic optimization, the high ambient temperature poses several practical design challenges. One is that material strengths are lower than at room temperature. Figure 3 below shows for instance the ultimate strength of austenitic stainless steels [3] as compared to their room temperature values. It can be seen that at temperatures around 200 °C, the ultimate strength is only about 70 % of that at room temperature. This needs to be incorporated in the design of parts and welds. Because of the limited experience with these conditions, we also chose to qualify the most critical welds under corresponding conditions, as presented in the next chapter.

Another significant impact is that on the performance characteristics of materials. Permanent magnet materials have an upper temperature limit, the so-called Curie temperature, above which the magnets will be permanently demagnetized. For permanent magnet materials based on rare-earth metals (e.g. NeFeB magnets) the curie temperature depends on the grade of material used. The highest grade materials have the lowest temperature limit. So the linear motor design needs to be optimized with a suitable permanent magnet material.

Electrical resistivity in the coil wires is a major contributor to the conversion efficiency of the compressor. The resistivity of copper increases with temperature. A typical temperature coefficient for copper is $4 \cdot 10^{-3}$ K^{-1}. This means that an increase in coil temperature of 150 K leads to an increase of 60 % in resistance, and thus also an increase in dissipation of 60 % in the coils for the same current. The coils need to be designed to accommodate this additional dissipation to prevent thermal runaways. In the qualification models, the coils have been fitted with temperature sensors near the windings to measure this effect.

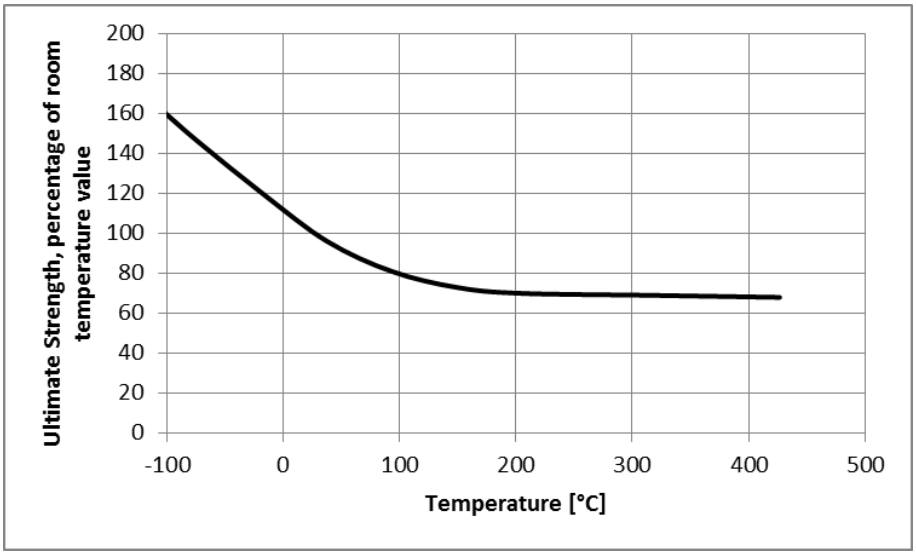

Figure 3: Ultimate strength versus temperature for austenitic stainless steels as a percentage of the room-temperature value.

TEST AND QUALIFICATION RESULTS

Process qualifications

Because of the high ambient temperatures many processes needed to be qualified for this. In particular the qualification of the weld strengths and the fatigue qualification of the springs will be presented below.

The yield and ultimate strength of metals will reduce at high ambient temperatures. In figure 3 above, the ultimate strength of austenitic stainless steels is plotted. It can be seen that at 200 °C ambient temperature, the yield strength of typical austenitic stainless steels is about 70 % of its room temperature value.

This has been accommodated in the design. To verify that the correction factors are sufficient, the weld strength has also been tested. The welds with the lowest margin of safety have been tensile tested at 200°C to validate. In figure 4 (left), the test sample is shown in the temperature chamber. In figure 4 (right), the results are shown. The breakage force on both samples corresponds and confirms the resulting margin of safety for the welds.

In a similar fashion, the fatigue limit of helical springs was investigated. A new material was used with a higher temperature limit. Due to the limited heritage with this new material, the fatigue limits of the material were tested. The goal of the test was to determine a statistically significant limit up to which the springs could be safely used.

The test protocol consisted of tests at increasing amplitude. Multiple springs were put on test, starting at relatively low amplitude. After $2 \cdot 10^6$ cycles, which is considered to be beyond 'infinite life' in fatigue testing, the amplitude was increased until one of the springs in the batch failed. At that point, a new spring is inserted and the test is recommenced at a lower amplitude. Two batches were tested, one with an additional thermal treatment to further improve the fatigue strength.

The test results give a sample population of springs with each a specific failure amplitude. These results were analyzed using the Weibull distribution, using the SuperSmith software package [4]. This analysis is comparable to lifetime testing, with the lifetime parameter replaced by amplitude.

The result is shown in figure 5 for the two batches. The 'characteristic amplitude' (Eta) is the amplitude at which 63% of the springs will not reach infinite life. The shape factor 'beta' for both data sets is high, which confirms fatigue as the failure mechanism. With this Weibull fit, the probability of failure of a spring at a certain stress can be calculated. The impact of the additional thermal treatment on the fatigue limit is clear; the characteristic amplitude increased from 4.2mm to 5.5mm. Therefore it was chosen to use these springs for the final design, with a sufficiently low failure probability due to fatigue.

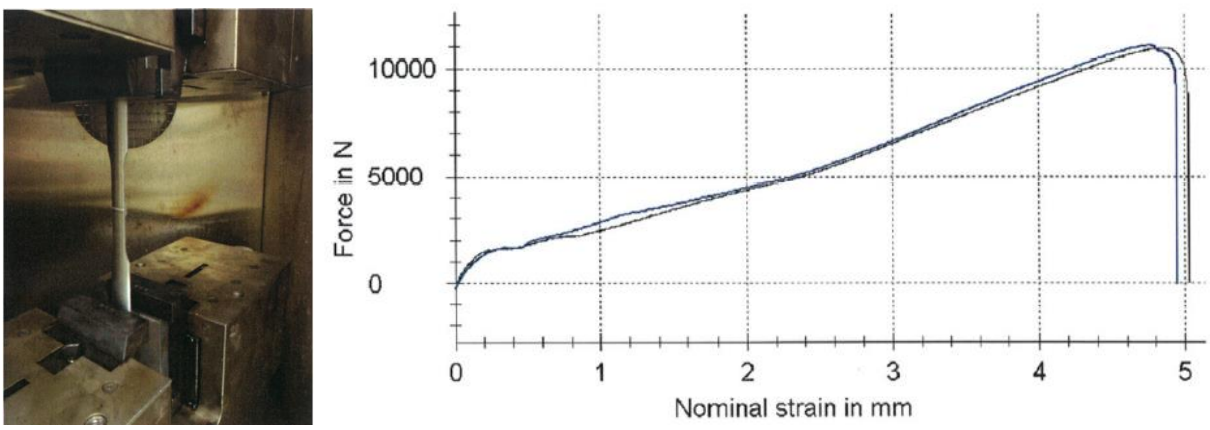

Figure 4: Tensile sample in test chamber (left) and tensile test results on two samples.

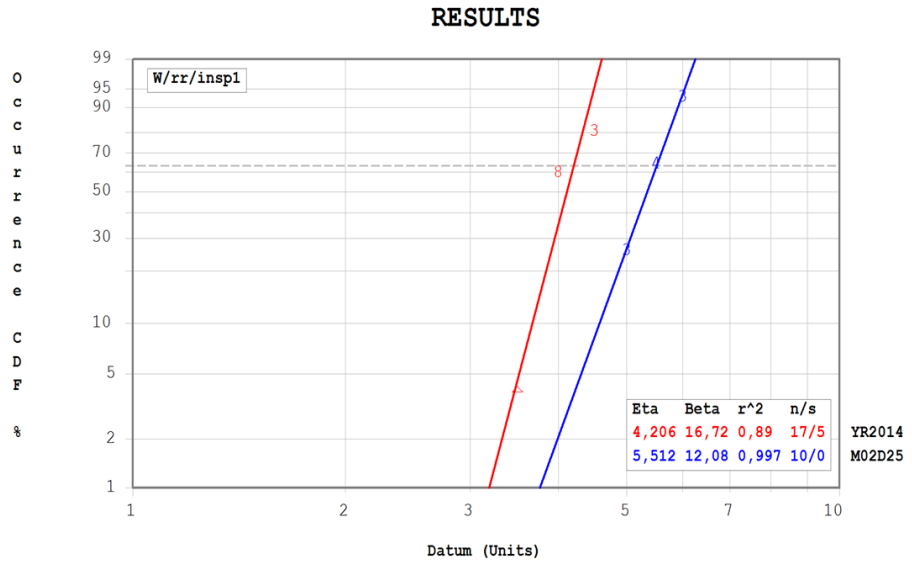

Figure 5: Weibull fit on spring failure versus amplitude. The blue curve is the spring design with additional heat treatment.

Performance testing

A full performance mapping as part of the qualification was done on two qualification models. The coolers were placed in a temperature chamber with the correct ambient temperature (figure 6).

The performance mapping was done over a range of chamber temperatures, tip temperatures, and input powers. The results of the mapping are shown in figure 7. The cooling power at 223 K is plotted versus the electrical input power for different ambient temperatures. Both qualification models reach the required cooling power of 25 W at 150 °C ambient temperature. The difference between the two models is less than 10%. This is also visible in figure 8 where the cooling power is plotted versus the tip temperature, at 150 °C ambient temperature and 175 W of electrical input power for both qualification models.

In order to validate the thermal management of the cooler, the compressor coils were fitted with temperature sensors. With these Pt-1000 sensors, placed on the windings, the temperature of the coils was monitored. In figure 9 below, the coil temperature SN1 is plotted versus the input power for different ambient temperatures. It can be seen that the coil temperature is proportional to the ambient temperature and the input power. There is no sign of thermal runaway at higher input powers or higher ambient temperatures.

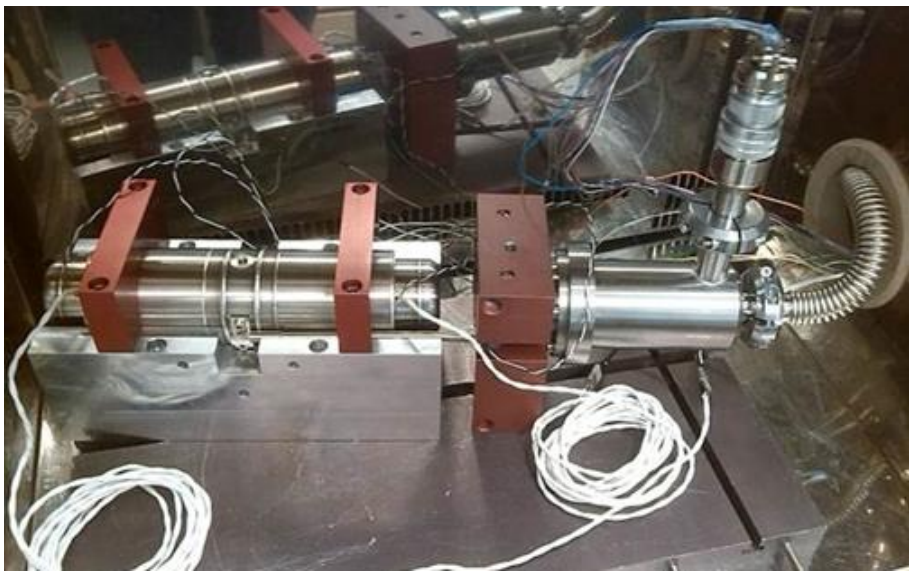

Figure 6: Photograph of one of the qualification models in the climate chamber.

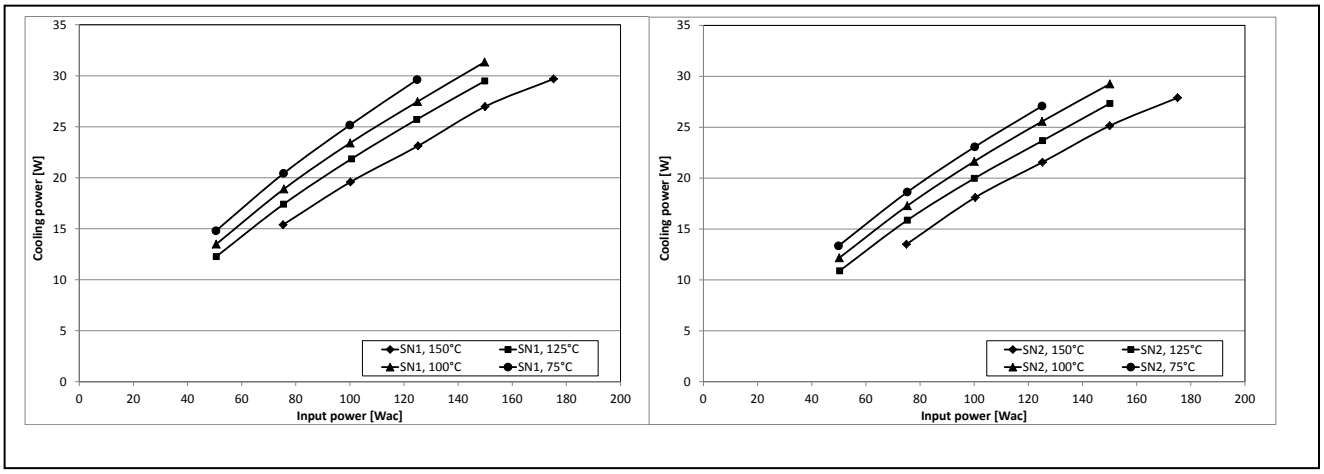

Figure 7: Cooling power versus input power at 223 K tip temperature for different ambient temperatures. Left graph is the result for the first qualification model, right graph for the second.

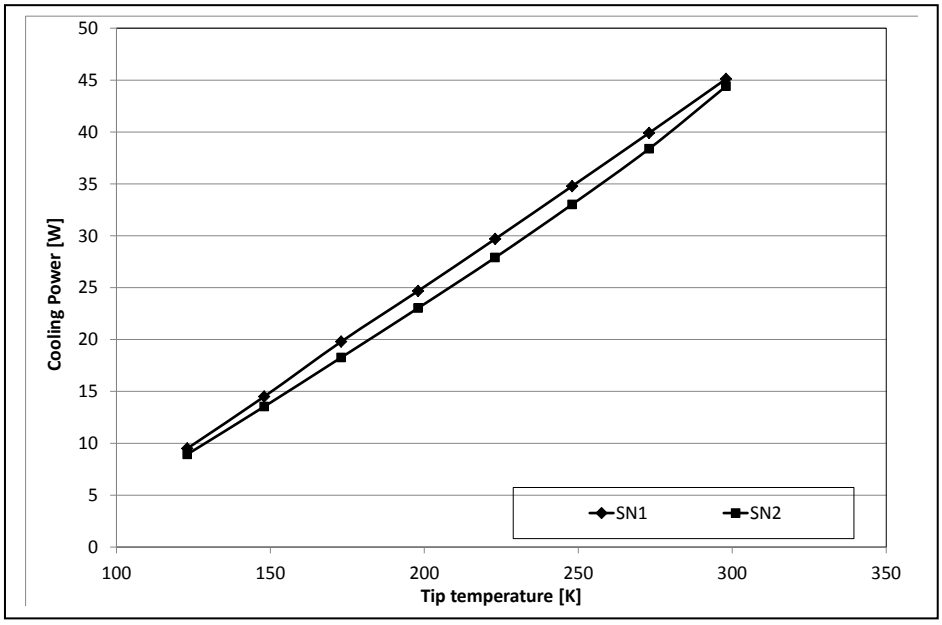

Figure 8: Cooling power versus tip temperature, 150°C ambient temperature and 175W input power.

Environmental testing

The mechanical environment for the cooler is characterized by a shock requirement and a random-vibration requirement. The cooler was tested at TCBV for the random vibration testing. The testing was done at ambient temperature. The qualification spectrum (shown in figure 10) adds to a total acceleration of 10 g_{rms}. The cooler was subjected to this spectrum for 2 hours in each axis (three axes in total).

The cooler is shown in the vibration jig, mounted on the shaker in figure 10. The cooler was not operating while tested. The performance criteria for pass fail were no degradation in performance and no helium leak. Both targets were reached.

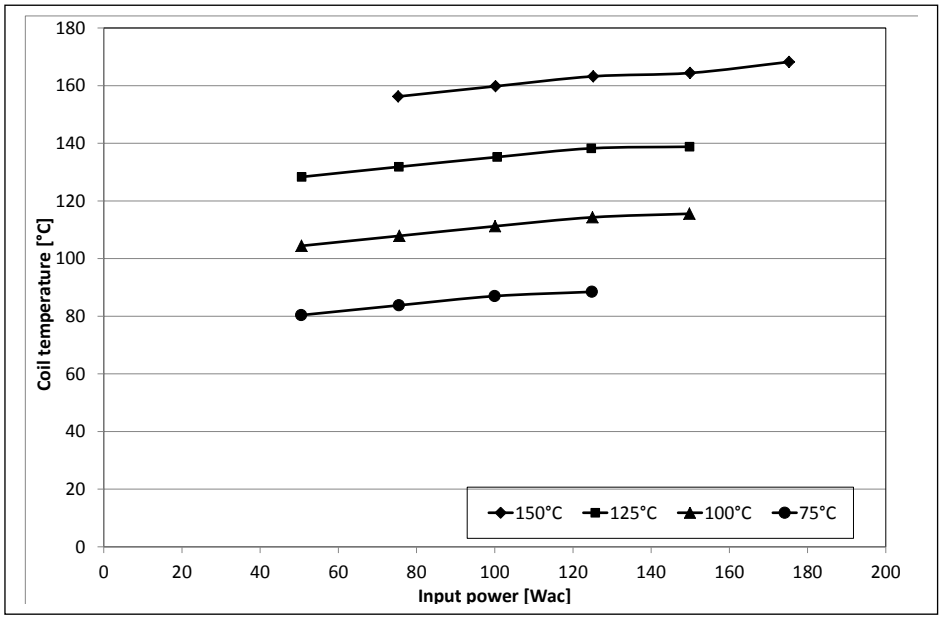

Figure 9: Coil temperature versus input power for different ambient temperatures.

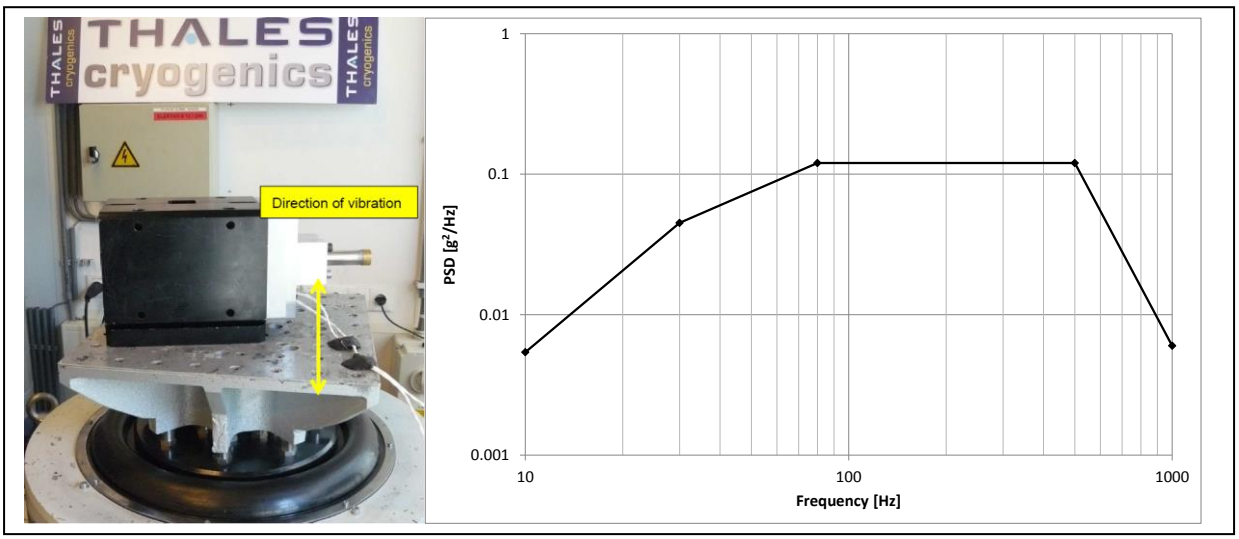

Figure 10: Cooler mounted on the shaker table (left). The compressor is completely encased in the jig; the cold finger protrudes on the right side. The graph on the right represents the qualification spectrum, corresponding to a total acceleration of 10 g_{rms}.

Series performance

After the qualification models, several small production batches were built. In total, 20 coolers were built. The performance of these coolers was monitored. In Figure 11 below, the cooling power at 150 °C ambient temperature, 223 K tip temperature, and four different input powers is plotted for all these coolers.

Some variation is present between individual models. The variation is approximately 10% around the average value, which is expected for coolers that are built in small series and use a lot of manual handling during testing. It can also be seen that there is a slightly increasing performance for the later models, corresponding to a better dialed-in production process.

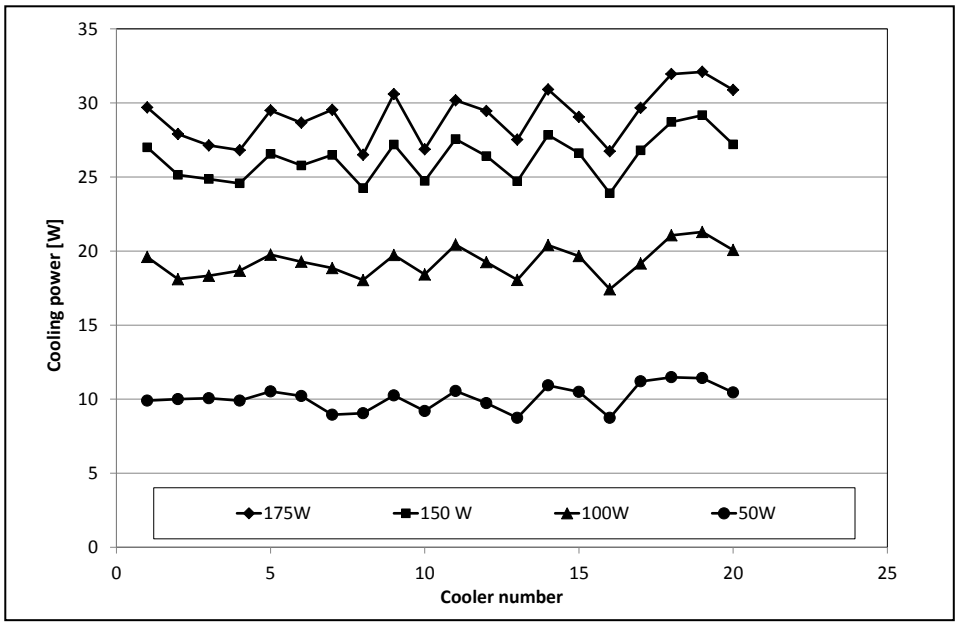

Figure 11: Cooling power at 150 °C ambient temperature and 223 K tip temperature, 4 input powers, for all the total production series.

CONCLUSIONS

A linear Stirling cooler was successfully built, tested, and qualified for use in applications with extreme ambient temperatures. The application is the cooling of sensors and electronics in a down-hole inspection tool for oil wells.

The application requires cooling at high ambient temperatures (150 °C), but at a similar temperature difference as in typical cryogenic application. As this results in an increased Carnot efficiency, it thus turned out that the thermodynamic optimization of the cooler was not the main challenge. On the other hand, the impact of the high ambient temperature on available material choices and their performance was large. The main challenge was in the material and process selection and associated qualifications.

The performance testing proved that the cooler met the requirements. The cooler has been industrialized to be built in small series. Up to now 20 coolers have been built, showing consistent performance throughout the different production batches.

REFERENCES

[1] R. Arts, D. Willems, J. Mullié, R. van Leeuwen, P. Bollens, G. de Jonge, T. Benschop, “Robust Stirling coolers for sensing in extreme environmental conditions”, Proceedings of SPIE, to be published.

[2] A.T.A.M. de Waele, P.P. Steijaert, J. Gijzen, “Thermodynamical aspects of pulse tubes”, Cryogenics 37 (1997), pp. 313-324.

[3] MIL-HDBK-5, Department of defence handbook: Metallic materials and elements for aerospace vehicle structures

[4] Supersmith Weibull.